











# Influence of induced drought on photosynthetic performance in *Dactylis glomerata* varieties during the early growth stage

Barbara Borawska-Jarmułowicz\*<sup>1)</sup>  , Grażyna Mastalerczuk<sup>1)</sup>  ,  
Piotr Dąbrowski<sup>2)</sup>  , Żaneta Tuchowska<sup>1)</sup>  , Hazem Kalaji<sup>3)</sup>  

<sup>1)</sup> Warsaw University of Life Sciences – SGGW, Institute of Agriculture, Nowoursynowska St, 159, 02-776 Warsaw, Poland

<sup>2)</sup> Warsaw University of Life Sciences – SGGW, Institute of Environmental Engineering, Nowoursynowska St, 159, 02-776 Warsaw, Poland

<sup>3)</sup> Institute of Technology and Life Sciences – National Research Institute, Falenty, Hrabska Ave, 3, 05-090 Raszyn, Poland

\* Corresponding author

RECEIVED 26.08.2023

ACCEPTED 25.01.2024

AVAILABLE ONLINE 29.03.2024

**Abstract:** Drought significantly impacts the growth and yield of forage grasses, particularly its effect on *Dactylis glomerata* photosynthetic apparatus during the initial phase of development remains largely unknown. This study investigated the effects of drought on physiological parameters of various *D. glomerata* varieties. The seedlings obtained after seed germination under optimal and simulated drought conditions by PEG 6000 (three variants) were planted in small pots filled with garden substrate. Over a span of 42 days, the plants were initially kept well-watered (70% capillary water capacity, CWC), after which half of the seedlings from each variant were subjected to drought. This drought stress was applied during the tillering phase for 12 days. Subsequently, the plants were rehydrated (at 70% CWC) and allowed to recover for 14 days. Throughout both drought and recovery periods, measurements were taken. Leaf chlorophyll fluorescence parameters were assessed, and the JIP-test analysis was utilised to provide detailed insights into the functionality of *D. glomerata* photosynthetic apparatus under drought stress and post-recovery conditions. Several parameters were identified as indicative of the plants' sensitivity to drought, such as performance indices  $PI_{ABS}$  and  $PI_{tot}$ , along with quantum yield parameters  $\Psi_{E_0}$ ,  $\Phi_{E_0}$ , and  $\Phi_{P_0}$ . The results highlighted that var. Minora and Tukan exhibited greater tolerance to water deficit when compared to the other varieties studied. They showed a large increases in  $PI_{ABS}$  and  $PI_{tot}$  values after drought stress as well as after the re-watering (recovery period) compared to control plants. This suggests their potential for better adaptation to drought conditions.

**Keywords:** chlorophyll *a* fluorescence transient, *Dactylis glomerata*, JIP-test, tillering phase, water deficit

## INTRODUCTION

Amidst the context of climate change, water scarcity stands as a pivotal environmental factor that profoundly impacts plant development and yield conditions (Elsheery and Cao, 2008; Staniak and Kocoń, 2015; Omar *et al.*, 2018). The repercussions of drought on grass growth exhibit significant variation, even within the same species (Mastalerczuk, Borawska-Jarmułowicz and Kalaji, 2017). *Dactylis glomerata* varieties play a crucial role in fodder grass mixtures across both permanent and temporary grasslands within temperate climate settings (Borawska-Jarmułowicz, Mastalerczuk and Janicka, 2016; Borawska-Jarmułowicz

*et al.*, 2022). This species demonstrates robust growth after seeding and strong competitiveness in relation to other mixture components throughout subsequent years of utilisation, along with notable drought tolerance during later stages of development.

The increasing prevalence of prolonged droughts has had a discernible impact on grassland productivity in Poland (Gabryszuk, Barszczewski and Wróbel, 2021). This can be attributed to disruptions in plant metabolism, particularly the photosynthetic activity (Kalaji *et al.*, 2016; Fariaszewska *et al.*, 2017). The measurement of chlorophyll *a* fluorescence (ChlF) parameters, closely linked to PSII functionality (Baker and

Rosenqvist, 2004), has revealed responses to various stressors, including drought (Li *et al.*, 2006; Elsheery and Cao, 2008; Kalaji *et al.*, 2012; Kosmala *et al.*, 2012; Borawska-Jarmulowicz *et al.*, 2014; Guidi *et al.*, 2016; Sousa de *et al.*, 2017; Elsheery *et al.*, 2020). The non-destructive analysis of the polyphasic fast chlorophyll transient, developed for assessing photosynthetic function, involves recording chlorophyll fluorescence emitted by a dark-adapted leaf during a brief (typically one-second) pulse of intense actinic light using a fluorimeter (Strasser, Tsimilli-Michael and Srivastava, 2004). High-resolution measurements of chlorophyll *a* fluorescence transient offer a swift means of extracting comprehensive information about PSII photochemical activity. Fast ChlF induction, a non-invasive spectroscopic technique, facilitates the detection and measurement of the effects of photosynthesis inhibitors *in vivo* (Baker, 2008).

The augmentation of ChlF intensity upon continuous bright light application to a dark-adapted sample is time-dependent and serves as a basis for calculating fast ChlF kinetics data. These data yield the ChlF transient curve (Schansker, Toth and Strasser, 2005; Stirbet and Govindjee, 2011). The ChlF method holds potential for genotypic screening for drought tolerance (Guha, Sengupta and Reddy, 2013). Evaluating plant vitality under stress conditions is feasible through analysis of the ChlF transient curve. Fluorescence parameters obtained from this curve, known as JIP-test (Force, Critchley and Rensen van, 2003; Strasser, Tsimilli-Michael and Srivastava, 2004), rapidly identify the influence of diverse stress factors on photosynthesis and demonstrate PSII functionality (Schansker, Toth and Strasser, 2005; Oukarroum *et al.*, 2007). Chlorophyll fluorescence measurements, encompassing induction kinetics studies in dark-adapted samples followed by OJIP analysis, are commonly employed to study plant responses to abiotic stresses (Kalaji *et al.*, 2016).

A typical fluorescence transient show cases phases including the initial ( $F_0$ ), represented on the fluorescence transient curve as O, followed by J (~2 ms), I (~30 ms), culminating in maximal ( $F_M$ ) fluorescence (termed step P) (Strasser, Srivastava and Tsimilli-Michael, 2000; Strasser, Tsimilli-Michael and Srivastava, 2004). In photosynthetic samples kept in darkness, the electron acceptor side of PSII predominantly resides in the oxidised state (PSII reaction centres open, fluorescence intensity minimal). The swift O to J rise, referred to as the photochemical phase, is highly dependent on exciting light intensity, while the J-I and I-P segments of the fluorescence curve, known as thermal phases (temperature-sensitive), are much slower. Within less than 1 s, Chl *a* fluorescence reaches peak P.

The principal values are utilised to compute JIP-test parameters elucidating energy fluxes within and around the photosystem II (PSII) reaction centre (RC) (Strasser, Srivastava and Tsimilli-Michael, 2000). These parameters, expressed per active RC, denote specific energy fluxes, while per excited CS, they signify phenomenological energy fluxes. This framework enables evaluation of consecutive energy fluxes: average photon absorption (ABS), energy dissipation (DI), exciton trapping (TR), electron transport (ET), and reduction in electron acceptors at PSI's acceptor side (RE) for assessing PSII functions. Other widely used parameters for providing insights into plant state under drought include the performance index (PI) and Fv/Fm (Force, Critchley and Rensen van, 2003; Živcák *et al.*, 2008).

While *D. glomerata* is recognised as drought-tolerant during later development stages, scant attention has been paid to its early

growth phase photosynthetic behaviour under drought stress. Our prior research demonstrated that induced drought conditions during seed germination positively impacted the photosynthetic efficiency and morphological characteristics of *D. glomerata* seedlings amid soil water deficit (Borawska-Jarmulowicz *et al.*, 2020). This study employs the OJIP transient coupled with the JIP-test to uncover alterations in photosynthetic behaviours of *D. glomerata* plants during the tillering phase under drought conditions.

This study's objective is to unveil insights into the photosynthetic apparatus functions of *D. glomerata* plants in the early growth stage under drought stress. Furthermore, it seeks to determine if seedlings obtained from seeds germinated under simulated drought conditions influences chlorophyll fluorescence parameters in *D. glomerata* subsequent developmental phase (tillering phase), and to identify which fluorescence parameters could serve as clear indicators of water stress prompted by drought.

## MATERIALS AND METHODS

### PLANTS, GROWTH CONDITIONS AND EXPERIMENT DESIGN

The impact of drought stress on physiological parameters of seedlings from various Polish *Dactylis glomerata* varieties — Amera (early), Krysta, Minora (medium early), and Tukan (medium late) — sourced from Poznańska Hodowla Roślin Ltd., was systematically investigated. The seedlings were obtained after seed germination under optimal and simulated drought conditions. Seed germination was conducted on Petri dishes within a controlled phytotron environment, maintaining specific conditions: air humidity at 60–65%, temperature at 25/16°C (day/night), and a photoperiod of 8 h light and 16 h darkness, supplemented with a light intensity of 1000  $\mu\text{mol}\cdot\text{m}^{-2}\cdot\text{s}^{-1}$ . Drought conditions were replicated through polyethylene glycol (PEG) 6000 on four variations: 0.0 MPa (control with laboratory paper at 60% humidity using deionised water), -0.4, -0.8, and -1.2 MPa. Each variety underwent three replications per variant, adhering to the approach outlined by Hardegree and Emmerich (1994). The osmotic potential of each solution was measured utilising a cryoscopic osmometer Osmomat 030 (Gonotec, Germany).

After 21 days of germination, three replications of five plants each (seedlings possessing 2–3 leaves) from each variety of *D. glomerata* and induced variant of drought (during seed germination) were transplanted into pots (volume 1331  $\text{cm}^3$ ), filled with garden substrate. It was characterised by  $\text{pH}_{\text{KCl}}$  5.0–6.0, nitrogen content of 80–120  $\text{mg}\cdot\text{cm}^{-3}$ , available phosphorus ranging from 22–44  $\text{mg}\cdot\text{cm}^{-3}$ , and potassium within the range of 83–124  $\text{mg}\cdot\text{cm}^{-3}$ . Following this, a nitrogen fertilisation of 0.85 mg per pot (equivalent to 50  $\text{kg}\cdot\text{ha}^{-1}$ , applied as urea) was administered after 21 days of vegetation.

To maintain optimal conditions, the plants were watered every two days until the soil and pots reached the desired weight, thereby sustaining 70% capillary water capacity (CWC) over the course of the next 42 days. Subsequently, during the tillering phase (characterised by 1–2 shoots per plant), half of the seedlings from each variant were maintained at 70% CWC (serving as the control), while the other half were subjected to a drought with no

watering for 12 days. Following the drought period, re-watering was initiated, restoring optimum soil moisture (70% CWC) for an additional 14 days. Data collection occurred over four distinct time points: (1) at the commencement of the drought period, (2) after 7 days of drought conditions (7 DAT), (3) after 12 DAT, and (4) after 14 days of re-watering (14 DAR).

### PHYSIOLOGICAL MEASUREMENTS

Leaf chlorophyll fluorescence parameters were assessed utilising a portable chlorophyll fluorometer (Pocket PEA, DataPEA Plus Version: 1,10, Hansatech Instruments Ltd., England) following a 30-min period of dark adaptation for the plants. All measurements were executed within consistent phytotron conditions identical to the growth environment of the plants. The measurements were conducted in the tillering phase on the youngest fully expanded leaf of nine plants (three per replication) within each combination (variety, seed germination variant, and growth condition variant). The OJIP curve was derived from the mean values of these three measurements (with three replications for each combination).

To illuminate the intricate alterations in PSII behaviours throughout drought and subsequent re-watering phases in *D. glo-*

*merata* varieties, modifications in the phases within the relative variable fluorescence kinetics were scrutinised by doubly normalising the OJIP transients. In order to visually depict the impact of drought stress on the trajectory of the chlorophyll fluorescence induction curve, the relative variable fluorescence ( $V_t$ ) was calculated using the formula:  $V_t = (F_t - F_0)/(F_M - F_0)$ . The distinction in relative variable fluorescence curves stemming from drought stress was evaluated by contrasting the normalised fluorescence values (between O and P steps) observed in control plants under drought conditions (Strasser *et al.*, 2010).

The induction curve generated was further used for the computation of various parameters signifying PSII performance. Specific energy fluxes for individual PSII reaction centres (RCs) and phenomenological energy fluxes assessed for the photosynthetic sample's area ( $C_S$ ) at  $t = 0$  were determined, alongside performance indices calculated on an absorption basis ( $PI_{ABS}$ ,  $PI_{tot}$ ). Biophysical parameters were deduced from the OJIP transients, including quantum yields ( $\Phi_{P_0}$ ,  $\Phi_{E_0}$ ,  $\Phi_{R_0}$ ,  $\Psi_{E_0}$ ,  $\delta_{R_0}$ ), specific activities per reaction centre (RC), performance indices (PI), and structure-function indices ( $V_j$ ,  $S_m$ ,  $N$ ) (Strasser *et al.*, 2010). The descriptions and abbreviations of the employed fluorescence parameters are provided in Table 1.

**Table 1.** Definition of the selected fluorescence parameters (all fluorescence parameters are in relative units)

Parameter	Description
<b>Normalised data</b>	
$t_{FM}$	time (in ms) to reach the maximal fluorescence intensity $F_M$
$V_j = (F_j - F_0)/(F_M - F_0)$	relative variable fluorescence at the J-step at moment $t$ ( $t = 2$ ms); $F_j$ = fluorescence level at that moment; $F_0$ = minimal fluorescence level; $F_M$ = maximal fluorescence level
$S_m = (Area)/(F_M - F_0)$	normalised total area above the OJIP curve (reflecting multiple turnover of $Q_A$ reductions)
$N = S_m \cdot (M_0/V_j)$	number indicating how many times $Q_A$ is reduced until fluorescence reaches its maximal value $F_M$ (number of $Q_A$ redox turnovers until $F_M$ is reached)
<b>Specific energy fluxes (per primary electron acceptor in PSII) – Quinone A (<math>Q_A</math>) – reducing PSII reaction centre – RC)</b>	
$ABS/RC = (1 - \gamma RC)/\gamma RC$	absorbed energy flux per RC; absorption flux per one active RC, a ratio of active to inactive RCs
$DI_0/RC = (ABS/RC - R_0/RC)$	dissipated energy flux per RC (at $t = 0$ ); energy flux not intercepted by an RC, dissipated in the form of heat, fluorescence, or transfer to other systems, at time $t = 0$
$TR_0/RC = M_0(1/V_j)$	trapped energy flux per RC; energy flux trapped by one active RC at $t = 0$
$ET_0/RC = M_0(1/V_j)\Psi_{E_0}$	electron transport flux per RC; rate of electron transport by one active RC at $t = 0$
$RE_0/RC = M_0(1/V_j)(1 - V_I)$	electron flux reducing end electron acceptors at the PSI acceptor side per RC
<b>The quantum yield for primary photochemistry</b>	
$\Phi_{P_0} = 1 - F_0/F_M$	maximum quantum yield of primary photochemistry (at $t = 0$ )
$\Phi_{E_0} = (1 - F_0/F_M)(1 - V_j)$	quantum yield of electron transport (at $t = 0$ )
$\Phi_{R_0} = (1 - F_0/F_M)(1 - V_I)$	quantum yield of reduction of end electron acceptors at the PSI acceptor side (RE)
$\Psi_{E_0} = 1 - V_j$	probability (at $t = 0$ ) that a trapped exciton moves an electron into the electron transport chain beyond $Q_A^-$
$\delta_{R_0} = (1 - V_I)/(1 - V_j)$	efficiency/probability with which an electron from the intersystem electron carriers moves to reduce an electron acceptors at the PSI acceptor side (RE)
<b>Phenomenological fluxes</b>	
$ABS/CS_0$	absorbed energy flux per excited cross section ( $CS_0$ )
$DI_0/CS_0$	dissipated energy flux per $CS_0$
$TR_0/CS_0$	trapped energy flux per $CS_0$
$ET_0/CS_0$	electron transport flux per $CS_0$

cont. Tab. 1

Parameter	Description
$RE_0/CS_0$	electron flux reducing end electron acceptors at the PSI acceptor side per $CS_0$
$ABS/CS_m$	absorbed energy flux per cross section ( $CS_m$ )
$DI_0/CS_m$	dissipated energy flux per $CS_m$
$TR_0/CS_m$	trapped energy flux per $CS_m$
$ET_0/CS_m$	electron transport flux per $CS_m$
$RE_0/CS_m$	electron flux reducing end electron acceptors at the PSI acceptor side per $CS_m$
Performance indices	
$PI_{ABS} = \gamma RC / (1 - \gamma RC) \cdot \varphi_{P_0} / (1 - \varphi_{P_0}) \cdot \Psi_{E_0} / (1 - \Psi_{E_0})$	performance index (potential) for energy conservation from exciton to the reduction of intersystem electron acceptors calculated on the basis of absorption
$PI_{tot} = PI_{ABS} \cdot \delta_{R_0} / (1 - \delta_{R_0})$	performance index (potential) for energy conservation from exciton to the reduction of PSI end acceptors

Source: own elaboration based on: Strasser, Srivastava and Tsimili-Michael (2000), Strasser, Tsimili-Michael and Srivastava (2004), Strasser *et al.* (2010), and Tsimilli-Michael (2020).

## STATISTICAL ANALYSIS

Statistical analysis of the data obtained during drought period and recovery of plants in the tillering phase was conducted through a multifactor analysis of variance (ANOVA) using Statistica 13.3 software (Statsoft Inc., Tulsa, OK, USA). The experiment was replicated three times. The key experimental factors encompassed: (A) soil moisture during the plants growth (optimum, drought), (B) simulated drought during seed germination (0.0 MPa, -0.4 MPa, -0.8 MPa, and -1.2 MPa), (C) *D. glomerata* variety (Amera, Krysta, Minora, and Tukan), and (D) measurement term (1, 2, 3 – corresponding to drought period, and 4 – post-recovery period). Additionally, interactions between soil moisture (optimum and drought) and the PEG variant (germination conditions) were examined. To assess significant differences, the means of each evaluated parameter were compared using Tukey's HSD test at a significance level of  $p \leq 0.05$ . A principal component analysis (PCA) was performed to examine relationships between the tested parameters and characterise the multivariate distinctions among them in relation to the plant growth conditions.

## RESULTS AND DISCUSSION

### OJIP FLUORESCENCE TRANSIENTS AND CALCULATED CURVES

Drought stands as a significant factor capable of impeding plant functionality (Heerden van Swanepoel and Kruger, 2009). Despite numerous investigations aimed at unravelling the intricate mechanism through which drought stress influences plant photosynthesis, this subject remains an ongoing area of exploration (Lawson *et al.*, 2003). Furthermore, thus far, no research has been conducted to ascertain the potential impact of drought-induced changes in seeds (resulting from increased surface tension with PEG 6000) on the subsequent performance of the photosynthetic apparatus in sprouted seedlings, which inevitably operate within water deficit conditions. The mechanism constraining photosynthesis during water scarcity is intricate, particularly as drought escalates to severe levels. Our research indeed validated the hypothesis that seed hardening does

influence the ensuing resilience of *Dactylis glomerata* in the face of this stress. Nevertheless, the stress response was notably contingent on the variety in question and the duration of the drought (Tab. 2).

Throughout the examination, the tested *D. glomerata* varieties consistently exhibited typical OJIP chlorophyll fluorescence transients both during drought application and after plant recovery (Figs. 1–4). The trajectory of Chl *a* fluorescence transitions across the distinct phases O–J, J–I, and I–P directly correlated with the physiological state of the photosynthetic subject. Our conclusions indicated that when maintained at 70% CWC soil moisture (as a control), no discernible alterations in the OJIP curve's trajectory were observed. However, following drought stress, the values of OJIP-test parameters exhibited clear discrepancies among the studied varieties, contingent upon the specific accession. As per Baker (2008), drought stress has the potential to alter the characteristic points of the OJIP curve and lead to a reduction in fluorescence intensity at the J, I, and P steps. However, the extent of this change is variably influenced by the specific plant variety. Our observations align with this notion, revealing that the application of drought induced a reduction in the progression of induction curves across all tested plants, in comparison to the control. Particularly, the I–P phase bore the brunt of this impact, which can be attributed to a decline in electron acceptors. Similar phenomena were documented by Oukarroum *et al.* (2007) in barley plants. Stirbet and Govindjee (2012) elucidate that during the J–I–P phase, PSII reaction centres gradually close while the plastoquinone pool concurrently experiences reduction.

In our investigation, plants of var. Amera, originating from seeds germinated under induced drought conditions of -1.2 MPa, then subjected to 12 days of drought, exhibited a curve with a steeper trajectory than those of the other conditions. Notable disparities were evident at points I and P (Fig. 1B). Conversely, the curves obtained for the remaining variants closely resembled the trajectory of plants not subjected to stress. After recovery under 70% CWC conditions, it remained apparent that the curve generated for plants originating from seeds germinated under -1.2 MPa drought maintained the steepest course (Fig. 1D). All these shifts predominantly occurred within the last section of

**Table 2.** Significance of the effect of factors and their interactions on the analysed variables based on the analysis of variance

Parameter	Soil moisture (A)		Induced drought – during seed germination, MPa (B)				Variety (C)				Term of measurement (D)				AxB	AxC	AxD	BxC	BxD	CxD	AxBxC	AxBxD	AxCxD	BxCxD	AxBxCxD	
	O	D	0.0	-0.4	-0.8	-1.2	A	K	M	T	1	2	3	4												
$f(F_{M})$	b	a	ns	ns	ns	ns	ns	ns	ns	ns	ns	ns	ns	*	*	*	*	ns	*	*	*	*	*	*	*	*
$V_j$	ns	ns	ns	ns	ns	ns	ns	ns	ns	bc	b	c	a	ns	*	*	*	*	*	*	*	*	*	*	*	*
$S_m$	ns	ns	ns	ns	ns	ns	ns	ns	ns	ab	b	a	ab	ns	*	*	*	*	ns	*	*	*	*	*	*	*
N	ns	ns	ns	ns	ns	ns	ns	ns	ns	ns	ns	ns	ns	ns	ns	ns	ns	*	*	*	*	*	*	*	*	*
ABS/RC	ns	ns	ns	ns	ns	ns	ab	b	ab	a	b	b	a	ns	*	*	*	*	*	*	*	*	*	*	*	*
DL <sub>0</sub> /RC	ns	ns	ns	ns	ns	ns	ab	b	ab	a	c	ab	bc	a	*	*	*	*	*	*	*	*	*	*	*	*
TR <sub>0</sub> /RC	ns	ns	ns	ns	ns	ns	ns	ns	ns	ns	b	b	a	ns	*	*	*	*	*	*	*	*	*	*	*	*
ET <sub>0</sub> /RC	ns	ns	ns	ns	ns	ns	b	ab	ab	a	ab	b	a	ns	*	*	*	*	*	*	*	*	*	*	*	*
RE <sub>0</sub> /RC	ns	ns	b	a	a	ab	b	a	b	ab	b	a	ab	*	*	*	*	*	*	*	*	*	*	*	*	*
$\phi_{p_0}$	ns	ns	ns	ns	ns	ns	ab	a	ab	b	a	bc	ab	c	ns	*	*	*	*	*	*	*	*	*	*	*
$\Psi_{E_0}$	ns	ns	ns	ns	ns	ns	ns	ns	ns	ab	b	a	c	ns	*	*	*	*	*	*	*	*	*	*	*	*
$\phi_{p_5}$	ns	ns	ns	ns	ns	ns	ns	ns	ns	ns	a	b	a	c	ns	*	*	*	*	*	*	*	*	*	*	*
$\delta_{R_0}$	ns	ns	b	a	a	ab	bc	a	c	ns	ns	ns	ns	*	*	*	*	*	*	*	*	*	*	*	*	*
$\phi_{p_8}$	ns	ns	ns	ns	ns	ns	a	ab	a	b	a	b	a	ns	*	*	*	*	*	*	*	*	*	*	*	*
ABS/CS <sub>0</sub>	ns	ns	b	b	a	bc	a	bc	c	ab	a	b	b	*	*	*	*	*	*	*	*	*	*	*	*	*
DL <sub>0</sub> /CS <sub>0</sub>	ns	ns	ns	ns	ns	ns	ab	b	ab	a	ab	a	c	ns	*	*	*	*	*	*	*	*	*	*	*	*
TR <sub>0</sub> /CS <sub>0</sub>	ns	ns	b	b	a	b	a	b	c	ab	a	b	b	c	*	*	*	*	*	*	*	*	*	*	*	*
ET <sub>0</sub> /CS <sub>0</sub>	ns	ns	b	ab	a	b	a	a	b	a	a	b	b	c	*	*	*	*	*	*	*	*	*	*	*	*
RE <sub>0</sub> /CS <sub>0</sub>	ns	ns	c	b	a	bc	a	b	b	b	a	ab	b	c	*	*	*	*	*	*	*	*	*	*	*	*
ABS/CS <sub>m</sub>	ns	ns	b	b	a	b	a	a	b	a	a	b	c	d	*	*	*	*	*	*	*	*	*	*	*	*
DL <sub>0</sub> /CS <sub>m</sub>	ns	ns	b	b	a	b	a	bc	c	ab	a	b	b	b	*	*	*	*	*	*	*	*	*	*	*	*
TR <sub>0</sub> /CS <sub>m</sub>	ns	ns	ab	ab	a	b	a	a	b	a	a	b	c	d	*	*	*	*	*	*	*	*	*	*	*	*
ET <sub>0</sub> /CS <sub>m</sub>	a	b	ab	ab	a	b	a	a	b	a	a	b	b	c	*	*	*	*	*	*	*	*	*	*	*	*
RE <sub>0</sub> /CS <sub>m</sub>	ns	ns	ab	ab	a	b	a	ab	b	b	a	ab	c	c	*	*	*	*	*	*	*	*	*	*	*	*
PI <sub>ABS</sub>	a	b	a	b	ab	ab	ns	ns	ns	ns	a	a	b	b	*	*	*	*	*	*	*	*	*	*	*	*
PI <sub>tot</sub>	a	b	ns	ns	ns	ns	a	a	a	b	ab	b	a	c	ns	*	*	*	*	*	*	*	*	*	*	*

Explanations: soil moisture: O = optimum, D = drought; variety: A = Amara, K = Krysta, M = Minora, T = Tukan; term of measurement: 1 = beginning of drought, 2 = seven days after treatment of drought (7 DAT), 3 = 12 DAT and 4 = 14 days after re-watering (14 DAR). Abbreviations of fluorescence parameters see in Table 1; \* significant effect ( $p \leq 0.05$ ), a = the lowest value, d = the highest value, ns = not significant. Source: own study.

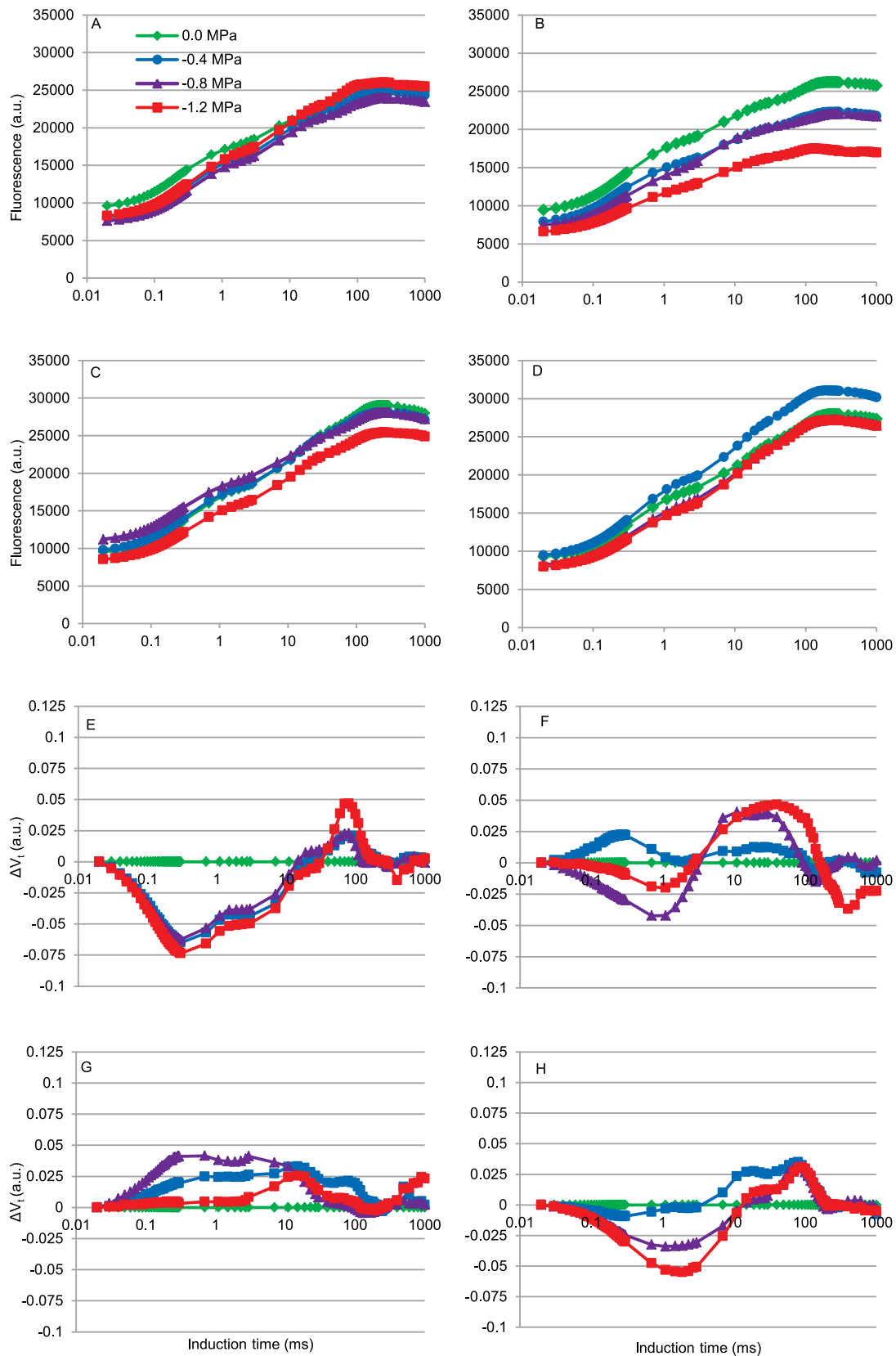


**Fig. 1.** Effect of drought on chlorophyll *a* fluorescence transients of dark adapted leaves of var. Amera; induction curves in 12 DAT (A – control, B – drought stress) and after re-watering (14 DAR) (C – control, D – recovery after drought); the fluorescence kinetics normalised – differential curves of  $\Delta V_t$  in 12 DAT (E – control, F – drought stress), and after re-watering (14 DAR) (G – control, H – recovery); 12 DAT = 12 days after treatment of drought, 14 DAR = 14 days after re-watering; values are means ( $n = 9$ ); double normalised curves presenting the relative variable fluorescence  $V_t$  in O–P transient of chlorophyll fluorescence; source: own study

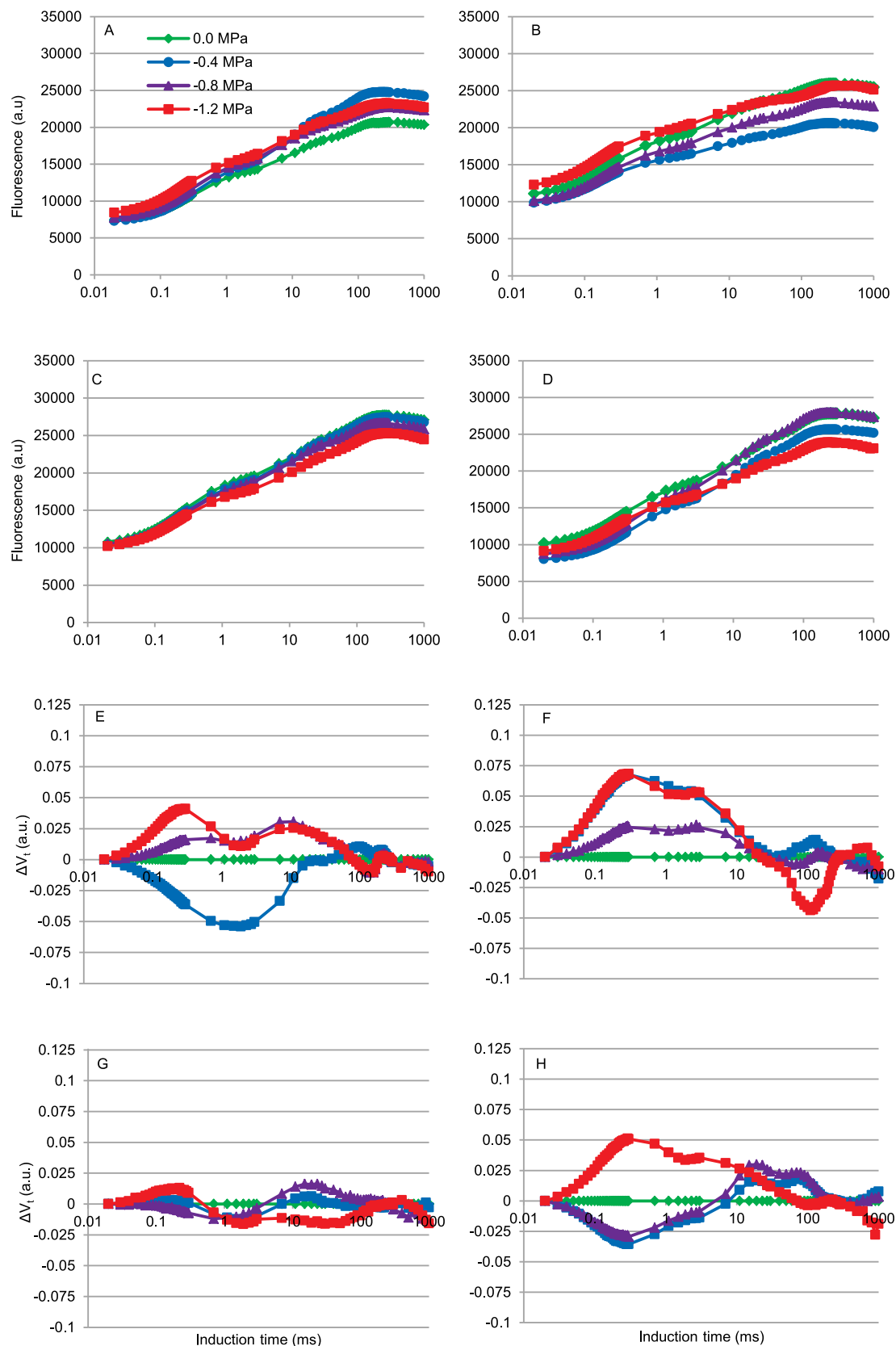


**Fig. 2.** Effect of drought on chlorophyll *a* fluorescence transients of dark adapted leaves of var. Krysta; induction curves in 12 DAT (A – control, B – drought stress) and after re-watering (14 DAR) (C – control, D – recovery after drought); the fluorescence kinetics normalised – differential curves of  $\Delta V_t$  in 12 DAT (E – control, F – drought stress), and after re-watering (14 DAR) (G – control, H – recovery); 12 DAT = 12 days after treatment of drought, 14 DAR = 14 days after re-watering; values are means ( $n = 9$ ); double normalised curves presenting the relative variable fluorescence  $V_t$  in O–P transient of chlorophyll fluorescence; source: own study

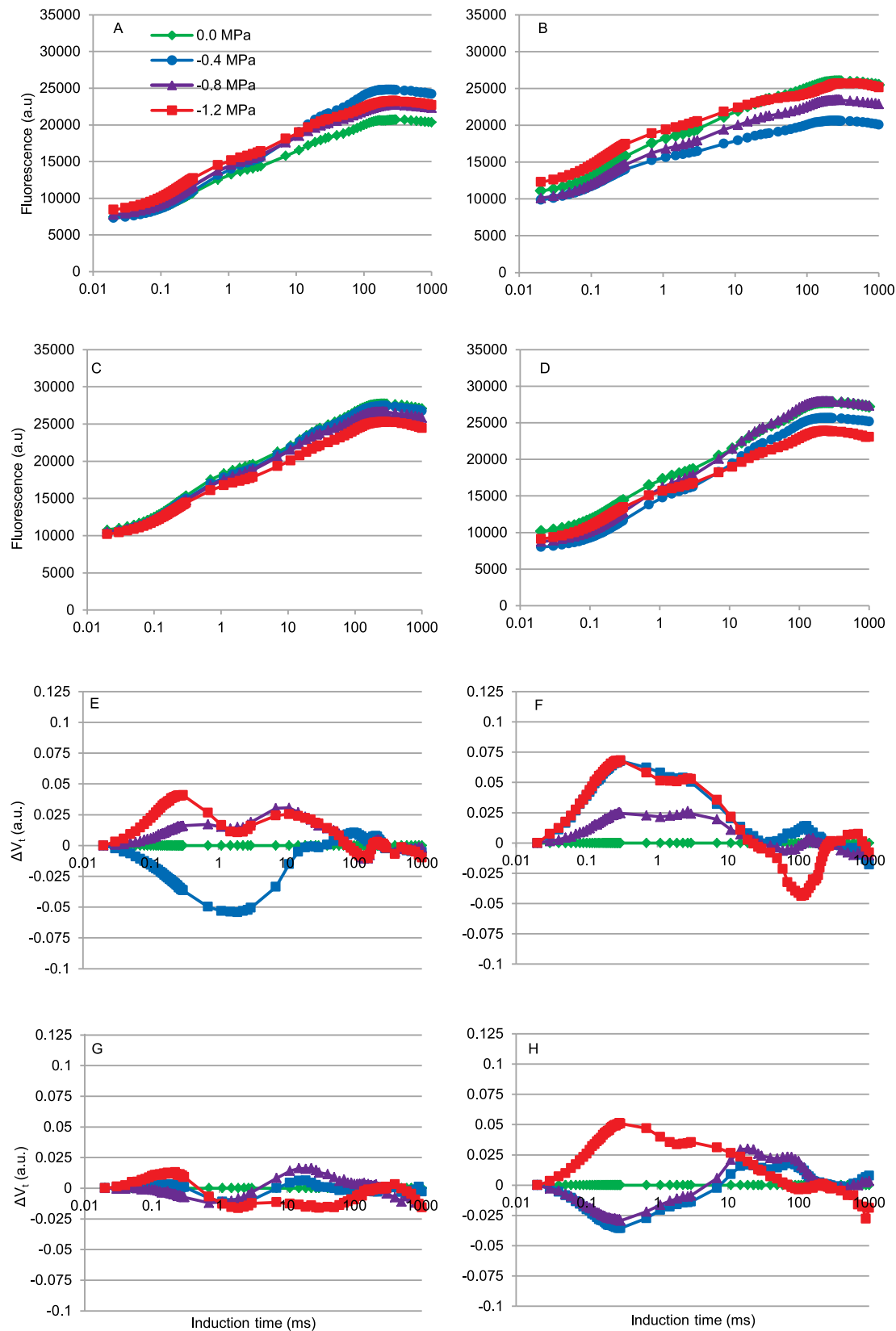


**Fig. 3.** Effect of drought on chlorophyll *a* fluorescence transients of dark adapted leaves of var. *Minora*; induction curves in 12 DAT (A – control, B – drought stress) and after re-watering (14 DAR) (C – control, D – recovery after drought); the fluorescence kinetics normalised – differential curves of  $\Delta V_t$  in 12 DAT (E – control, F – drought stress), and after re-watering (14 DAR) (G – control, H – recovery); 12 DAT = 12 days after treatment of drought, 14 DAR = 14 days after re-watering; values are means ( $n = 9$ ); double normalised curves presenting the relative variable fluorescence  $V_t$  in O–P transient of chlorophyll fluorescence; source: own study



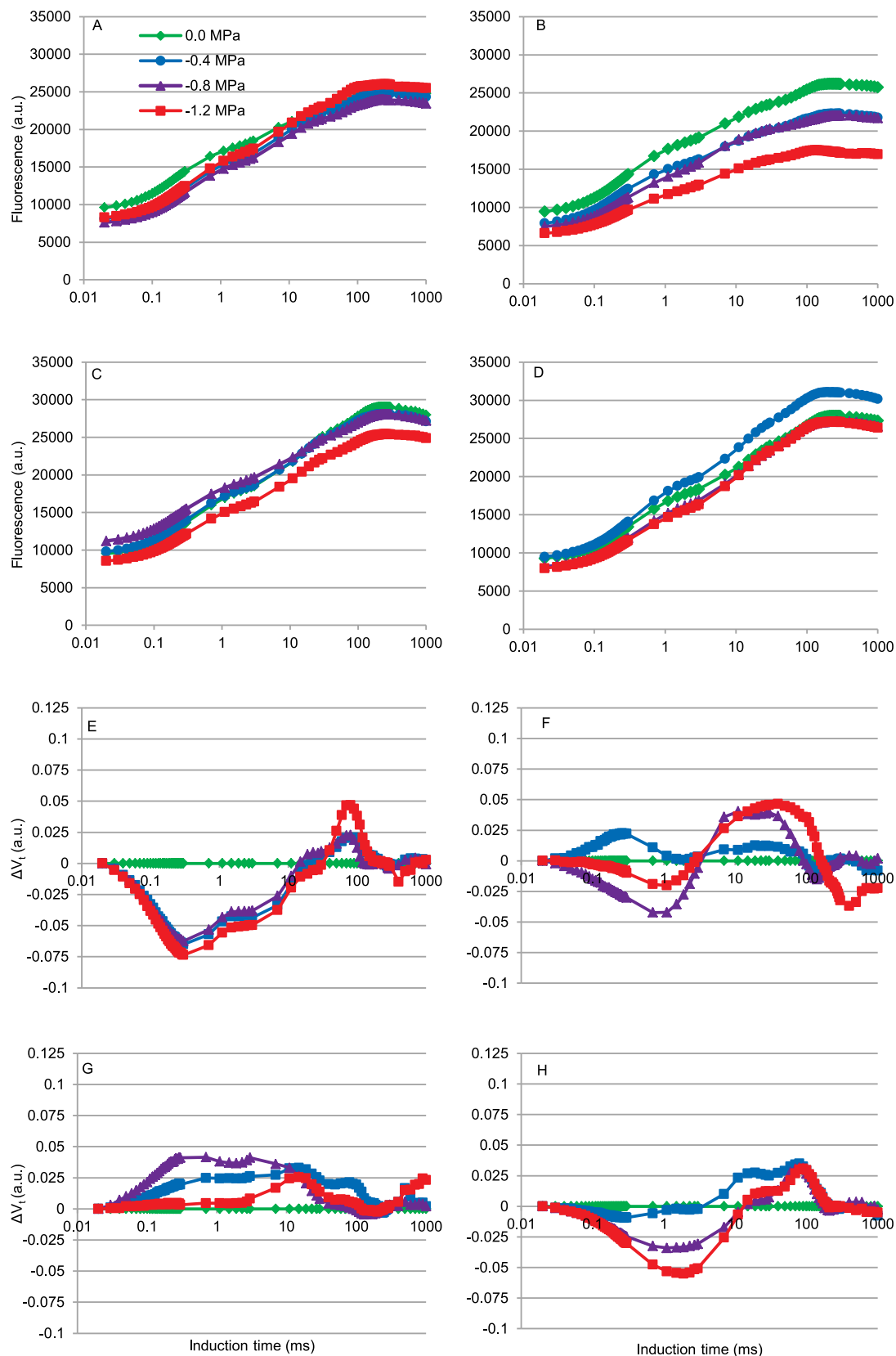


**Fig. 4.** Effect of drought on chlorophyll *a* fluorescence transients of dark adapted leaves of var. Tukan; induction curves in 12 DAT (A – control, B – drought stress) and after re-watering (14 DAR) (C – control, D – recovery after drought); the fluorescence kinetics normalised – differential curves of  $\Delta V_t$  in 12 DAT (E – control, F – drought stress), and after re-watering (14 DAR) (G – control, H – recovery); 12 DAT = 12 days after treatment of drought, 14 DAR = 14 days after re-watering; values are means ( $n = 9$ ); double normalised curves presenting the relative variable fluorescence  $V_t$  in O–P transient of chlorophyll fluorescence; source: own study

the curve, namely the I–P phase. Normalised curves affirm that the most significant variations in seedlings under drought stress emerged from plants whose seeds germinated under –1.2 MPa drought (Fig. 1E–H).

In the case of var. Krysta, alterations in the curve’s trajectory were observed after the conclusion of the drought phase, particularly in the J–I phase, termed as the thermal phase (spanning 2–30 ms), which is additionally influenced by PSI activity as outlined by Stribet and Govindjee (2012). Notably, changes were also apparent in the I–P section (Fig. 2B).

They were arranged higher in plants for variants 0.0 MPa and –1.2 MPa during seed germination. While plants maintained under the conditions of 70% CWC showed a lower course of curves for these variants of seed germination compared to –0.4 MPa and –0.8 MPa (Fig. 2A). After the recovery period, the curve for –1.2 MPa was much lower compared to other curves (Fig. 2D). At the same time similarly arranged curves were found for plants that were kept constantly under the conditions of 70% CWC (regardless of the variant of seed germination, Fig. 2C).

Under the influence of drought stress, there was a visible differentiation in the course of the curves also in Minora variety (Fig. 3).

In the I–P section, the trajectory of curves exhibited a higher course in plants stemming from the –1.2 MPa and 0.0 MPa germination variants, as opposed to plants originating from seeds germinated at –0.4 MPa and –0.8 MPa. Subsequent to the recovery period, the curve progression was consistent irrespective of the seed germination variant (Fig. 3D). Upon analysing the normalised curves, it can be deduced that the most pronounced alterations in seedlings subjected to drought stress were observed in cases where seeds had germinated under –0.8 MPa drought conditions. These changes were discernible across the O–J and J–I sections. Additionally, it was verified that plants deriving from

seeds treated with –1.2 MPa showcased the most robust recovery (Fig. 3E–H).

Concerning var. Tukan, upon the culmination of the 12-day drought period, it was evident that the curve progression across all variants was notably lower compared to the control (0.0 MPa) (Fig. 4). The most significant shifts (evident even within the O–J section) were observed in plants resulting from seeds treated with –1.2 MPa. For –0.4 MPa and –0.8 MPa variants, the curve progression was notably similar and exhibited higher values compared to the –1.2 MPa condition. The decrease in the maximal amplitude during the I–P phase implies a reduction in the PSI end electron acceptor pool size, potentially leading to an excessive reduction of the PSI acceptor side, as discussed by Kalachanis and Manetas (2010). Conversely, following the recovery period, the curve for the –0.4 MPa variant remained elevated compared to the others, with the overall course maintaining similarity. Analysing the normalised curves confirms that the most pronounced variations were observable in plants originating from seeds treated with –1.2 MPa (Fig. 4 E–H).

### JIP-TEST PARAMETERS CALCULATED FROM CHLOROPHYLL FLUORESCENCE TRANSIENTS

Although distinct alterations in the trajectory of OJIP curves were not evident across the varieties prior to the stress test, individual parameters of the JIP-test exhibited changes (Figs. 5–8).

Amid optimal soil moisture conditions (control, 70% CWC), the values of  $PI_{ABS}$  and  $PI_{tot}$  in var. Amera plants showcased an increase for the –0.4 MPa and –1.2 MPa germination variants, relative to the 0.0 MPa variant (Fig. 5A). However, upon the conclusion of the drought stress phase, the  $PI_{ABS}$  and  $PI_{tot}$  parameters exhibited a decrease, particularly pronounced in plants originating from seeds treated with

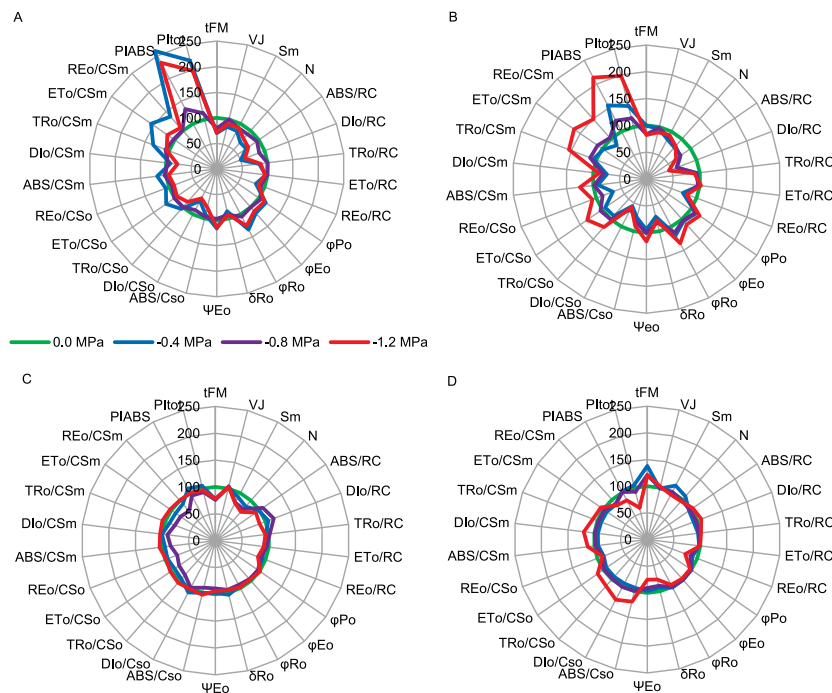


**Fig. 5.** A radar plot presentation of some important JIP-test parameters quantifying the behaviour of PSII of var. Amera in 12 DAT (A – control, B – drought stress) and after re-watering (14 DAR) (C – control, D – recovery after drought). All values are expressed in comparison to the values of control. Values are means ( $n = 9$ ); source: own study

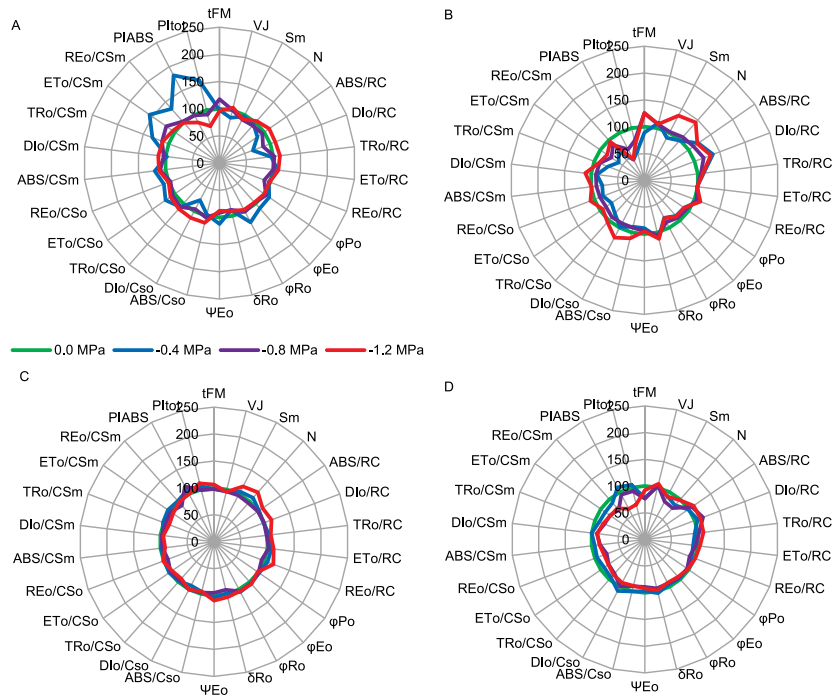


**Fig. 6.** A radar plot presentation of some important JIP-test parameters quantifying the behaviour of PSII of var. Krysta in 12 DAT (A – control, B – drought stress) and after re-watering (14 DAR) (C – control, D – recovery after drought). All values are expressed in comparison to the values of control. Values are means ( $n = 9$ ); source: own study

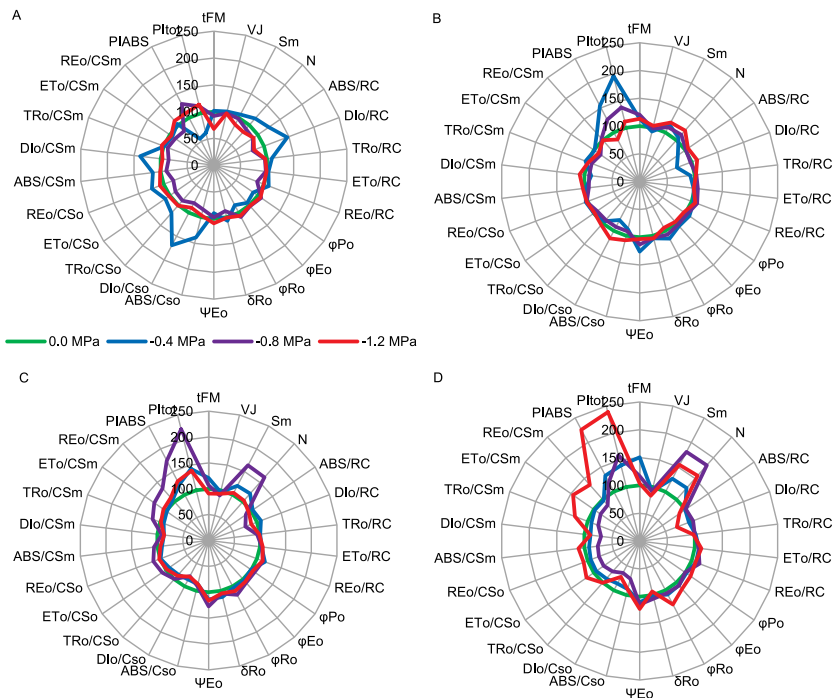


**Fig. 7.** A radar plot presentation of some important JIP-test parameters quantifying the behaviour of PSII of var. Minora in 12 DAT (A – control, B – drought stress) and after re-watering (14 DAR) (C – control, D – recovery after drought). All values are expressed in comparison to the values of control. Values are means ( $n = 9$ ); source: own study

-1.2 MPa. Nevertheless, these values remained elevated when compared to the 0.0 MPa condition.

Furthermore, it was discernible that heightened drought conditions (indicated by higher MPa values) during seed germination were associated with a reduction in ABS/RC in seedlings (Fig. 5B). Subsequent to the recovery period, plants

originating from seeds germinated under -1.2 MPa conditions displayed PI parameter values below that of the 0.0 MPa condition. Nevertheless, higher values were registered for several parameters, particularly phenomenological fluxes  $DI_0/CS_0$  and  $DI_0/CS_m$ , as well as the  $t(F_M)$  parameter (which was also observed across other seed germination variants) (Fig. 5D).

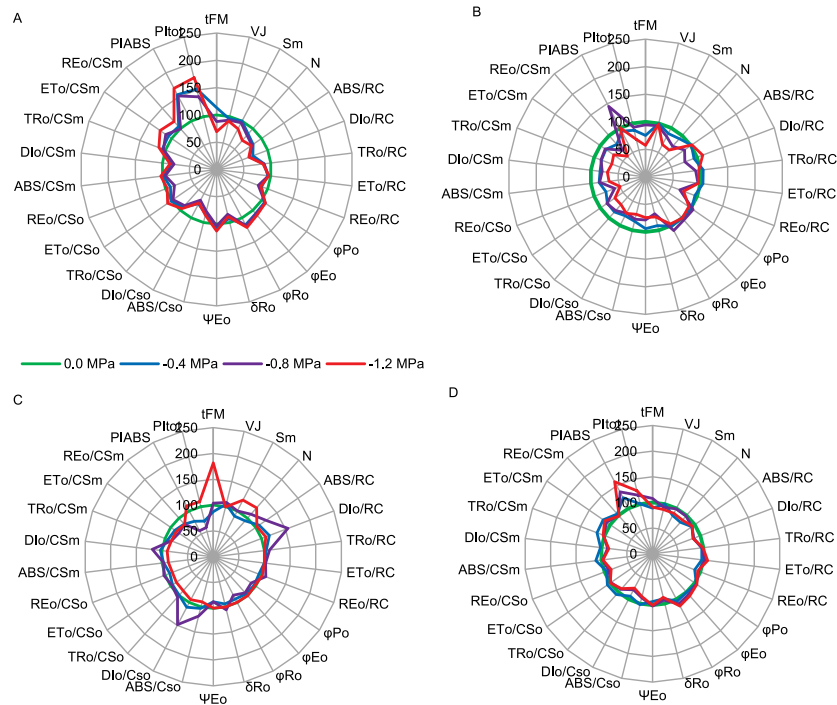


**Fig. 8.** A radar plot presentation of some important JIP-test parameters quantifying the behaviour of PSII of var. Tukan in 12 DAT (A – control, B – drought stress) and after re-watering (14 DAR) (C – control, D – recovery after drought). All values are expressed in comparison to the values of control. Values are means ( $n = 9$ ); source: own study

In the case of Krysta variety, under the conditions of optimum moisture (control, 70% CWC), elevated values were found for specific energy fluxes per primary electron acceptor in PSII –  $ET_0/CS_m$ ,  $RE_0/CS_m$ , along with performance indices  $PI_{ABS}$  and  $PI_{tot}$  solely in plants originating from seeds treated with  $-0.4$  MPa (Fig. 6A). However, following 12 days of drought, a decline in the values of parameters converted to  $CS_m$ , as well as  $PI_{ABS}$  and  $PI_{tot}$  was evident across all seed germination variants (Fig. 6B). Simultaneously, augmented values of  $S_m$  and  $N$  parameters were recorded in the  $-1.2$  MPa variant. After the plants underwent recovery, the majority of individual parameter values were generally lower in comparison to the control condition (0.0 MPa at 70% CWC), with a notable decline observed for  $PI_{ABS}$  and  $PI_{tot}$  indices (Fig. 6D).

Both  $PI_{ABS}$ , used to quantify PSII performance, and  $PI_{tot}$ , utilised to measure performance up to the reduction of PSI end electron acceptors, displayed remarkable sensitivity under drought conditions. Our study affirms that the  $PI_{ABS}$  parameter is among the most responsive within the JIP-tests for this particular type of stress. This aligns with conclusions drawn from the research conducted by Dąbrowski *et al.* (2019) on lawn varieties of *Lolium perenne* during drought. According to Zivčák *et al.* (2013), ChlF measurements suggest an enhanced safeguarding of PSII and PSI photochemistry under drought conditions through the adjustment of energy distribution between photosystems and the activation of alternative electron sinks.

In var. Minora, under control conditions (70% CWC), an elevation in the  $DI_0/RC$ ,  $DI_0/CS_0$ , and  $DI_0/CS_m$  parameters was discerned for the  $-0.4$  MPa variant (Fig. 7A). Following the drought period, augmented values were recorded for the  $PI_{ABS}$  and  $PI_{tot}$  parameters (vitality indices) in plants arising from seeds treated with  $-0.4$  MPa and  $-0.8$  MPa (Fig. 7B). Subsequent to the recovery period, higher values of  $PI_{ABS}$  and  $PI_{tot}$  were similarly

evident, particularly pronounced for the  $-1.2$  MPa variant (Fig. 7D). Conversely, among plants maintained under 70% CWC conditions, the highest values were observed for the  $-0.8$  MPa variant (Fig. 7C). It is noteworthy that both  $PI_{ABS}$ , employed to quantify PSII performance, and  $PI_{tot}$ , used to measure performance up to the reduction of PSI end electron acceptors, underwent modification due to drought stress. In var. Minora, substantial increments in the values of these indices were observed directly after the stress period, as well as following re-watering, when compared to control plants. This implies a more effective adaptation to drought conditions. Dąbrowski *et al.* (2019) demonstrated that performance index values significantly decreased following the application of drought stress in both varieties of *Lolium perenne*. Regardless of the variety and degree of drought, re-watering induced partial recovery of these parameters to the same values as in control plants. In our study, an increase in the values of  $S_m$  and  $N$  parameters was also evident (particularly for  $-0.8$  MPa and  $-1.2$  MPa).

In the case of Tukan variety, the application of induced drought during seed germination (from  $-0.4$  MPa to  $-1.2$  MPa) resulted in an increase in the values of the  $PI_{ABS}$  and  $PI_{tot}$  parameters under control conditions (Fig. 8A). Following the conclusion of the drought treatment, values for most parameters decreased across all variants, falling below the value observed for the 0.0 MPa condition. However, subsequent to the recovery period, values for the assessed parameters increased across all seed germination conditions and approached the levels of the 0.0 MPa condition (with  $PI_{ABS}$  and  $PI_{tot}$  values even surpassing the initial levels) (Fig. 8D). This pattern suggests, similar to the Minora variety, an enhanced adaptation to drought conditions.

After 7 days, the initial signs of stress emerged in the form of a reduction in the  $DI_0/RC$  parameter value. Subsequently, following 12 days of drought, a notable decline was observed in the values of



period exerted the most pronounced influence on the  $TR_0/RC$  parameter. Furthermore, strong positive correlations were identified among  $\Psi_{E_0}$ ,  $PI_{ABS}$ ,  $PI_{tot}$ , and  $\phi_{E_0}$ . Conversely,  $\phi_{P_0}$  exhibited a negative correlation with  $ABS/RC$  and  $DI_0/RC$  after the drought period. These parameters attained peak values in plants that originated from seeds germinated under the most severe drought conditions and subsequently underwent drought stress during the tillering phase ( $D\_MPa -1.2$ ). In contrast, optimal moisture conditions during the growth phase of plants derived from seeds germinated under drought conditions ( $O\_MPa -1.2$ ) favoured high  $\phi_{P_0}$  values.

Following the recovery period, the first principal component (PC1) now accounts for approximately 70.3% of the variability observed, while the second principal component (PC2) accounts for 14.7% (Fig. 9 C–D). Among the parameters, growth conditions continued to exert the most significant influence on  $TR_0/RC$  and  $DI_0/CS_0$ , which were positively correlated. Additionally, a strong positive correlation was identified between  $PI_{ABS}$  and  $PI_{tot}$  (performance indices),  $\Psi_{E_0}$ ,  $\phi_{E_0}$ , and  $\phi_{P_0}$  (parameters associated with quantum yield for primary photochemistry), as well as between  $V_j$  (normalised data),  $DI_0/RC$ , and  $ABS/RC$  (specific energy flux parameters) (Fig. 9C).

Performance indices and parameters linked to quantum yield for primary photochemistry reached their highest values under the  $D\_MPa -0.4$  conditions. Conversely, the highest values for specific energy flux parameters and  $V_j$  were registered under optimal soil moisture conditions (O) (Fig. 9D).

## CONCLUSIONS

In our study, we observed distinct responses of *Dactylis glomerata* varieties to drought stress. We identified several parameters that serve as indicators of reduced photosynthetic efficiency in these varieties when subjected to drought conditions. Notably, we reaffirmed that the  $PI_{ABS}$  parameter within the JIP-test framework is particularly sensitive to drought stress. Our investigation further demonstrated significant alterations in quantum yield parameters ( $\Psi_{E_0}$ ,  $\phi_{E_0}$ , and  $\phi_{P_0}$ ) across all tested *D. glomerata* varieties. These parameters are recognised for their accuracy in reflecting the impact of abiotic stresses, as they signify a decline in the efficiency of regulating the dissipation of excitation energy by the photosynthetic membrane. Additionally, specific energy flux parameters ( $DI_0/RC$  and  $ABS/RC$ ) also exhibited sensitivity to drought, although the degree of response varied among varieties. Notably, the Minora and Tukan varieties displayed greater tolerance to water deficit compared to other varieties as they showed a large increases in  $PI_{ABS}$  and  $PI_{tot}$  values after drought stress as well as after the re-watering (recovery period) compared to control plants. In summary, our data analysis underscores the complexity of the photosynthetic machinery's reaction to drought stress in *Dactylis glomerata*. Our findings highlight that drought-resistant varieties can maintain higher photosynthetic activity during drought stress. We have also established a correlation indicating that seed hardening plays a pivotal role in enhancing the subsequent drought resistance of plants in the tested varieties. Importantly, our study suggests that seed germination under drought conditions might enhance the efficiency of this process.

## CONFLICT OF INTERESTS

The authors declare no conflict of interests.

## REFERENCES

- Baker, N.R. (2008) "Chlorophyll fluorescence: A probe of photosynthesis in vivo," *Annual Review of Plant Biology*, 59, pp. 89–113. Available at: <https://doi.org/10.1146/annurev.arplant.59.032607.092759>.
- Baker, N.R. and Rosenqvist, E. (2004) "Applications of chlorophyll fluorescence can improve crop production strategies: an examination of future possibilities," *Journal of Experimental Botany*, 55(403), pp. 1607–1621. Available at: <https://doi.org/10.1093/jxb/erh196>.
- Borawska-Jarmułowicz, B. et al. (2022) "Effect of silicon-containing fertilizers on the nutritional value of grass-legume mixtures on temporary grasslands," *Agriculture*, 12, 145, Available at: <https://doi.org/10.3390/agriculture12020145>.
- Borawska-Jarmułowicz, B. et al. (2014) "Low temperature and hardening effects on photosynthetic apparatus efficiency and survival of forage grass varieties," *Plant, Soil and Environment*, 60, pp. 177–183. Available at: <https://doi.org/10.17221/57/2014-PSE>.
- Borawska-Jarmułowicz, B. et al. (2020) "Improving tolerance in seedlings of some Polish varieties of *Dactylis glomerata* to water deficit by application of induced drought during seed germination," *Photosynthetica*, 58 (SI), pp. 540–548. Available at: <https://doi.org/10.32615/ps.2020.007>.
- Borawska-Jarmułowicz, B., Mastalerczuk, G. and Janicka, M. (2016) "Ocena cech biologicznych oraz plonowania wybranych odmian *Dactylis glomerata*, *Festuca pratensis* i *Phleum pratense* w siewach czystych i mieszkach [Evaluation of biological characteristics and yield of selected varieties of *Dactylis glomerata*, *Festuca pratensis* and *Phleum pratense* in pure stands and mixtures]," *Łąkarstwo w Polsce*, 19, pp. 35–50.
- Dąbrowski, P. et al. (2016) "Prompt chlorophyll *a* fluorescence as a rapid tool for diagnostic changes in PSII structure inhibited by salt stress in perennial ryegrass," *Journal of Photochemistry and Photobiology, B: Biology*, 157, pp. 22–31. Available at: <https://doi.org/10.1016/j.jphotobiol.2016.02.001>.
- Dąbrowski, P. et al. (2019) "Exploration of chlorophyll *a* fluorescence and plant gas exchange parameters as indicators of drought tolerance in perennial ryegrass," *Sensors*, 19, 2736. Available at: <https://doi.org/10.3390/s19122736>.
- Elsheery, N.I. and Cao, K.F. (2008) "Gas exchange, chlorophyll fluorescence, and osmotic adjustment in two mango cultivars under drought stress," *Acta Physiologiae Plantarum*, 30, pp. 769–777. Available at: <https://doi.org/10.1007/s11738-008-0179-x>.
- Elsheery, N.I. et al. (2020) "Foliar application of nanoparticles mitigates the chilling effect on photosynthesis and photoprotection in sugarcane," *Plant Physiology and Biochemistry*, 149, pp. 50–60. Available at: <https://doi.org/10.1016/j.plaphy.2020.01.035>.
- Fariaszewska, A. et al. (2017) "Mild drought stress-induced changes in yield, physiological processes and chemical composition in *Festuca*, *Lolium* and *Festulolium*," *Journal of Agronomy and Crop Science*, 203, pp. 103–116. Available at: <https://doi.org/10.1111/jac.12168>.
- Force, L., Critchley, C. and Rensen van, J.J. (2003) "New fluorescence parameters for monitoring photosynthesis in plants," *Photosynthesis Research*, 78, pp. 17–33. Available at: <https://doi.org/10.1023/A:1026012116709>.
- Gabryszuk, M., Barszczewski, J. and Wróbel, B. (2021) "Characteristics of grasslands and their use in Poland," *Journal of Water and Land Development*, 51, pp. 243–249. Available at: <https://doi.org/10.24425/jwld.2021.139035>.

- Guha, A., Sengupta, D. and Reddy, A.R. (2013) "Polyphasic chlorophyll *a* fluorescence kinetics and protein analyses to track dynamics of photosynthetic performance in mulberry during progressive drought," *Journal of Photochemistry and Photobiology. B: Biology*, 119, pp. 71–83. Available at: <https://doi.org/10.1016/j.jphoto-biol.2012.12.006>.
- Guidi, L. *et al.* (2016) "Application of modulated chlorophyll fluorescence and modulated chlorophyll fluorescence imaging to study the environmental stresses effect," *Annali di Botanica*, 6, pp. 5–22. Available at: <https://doi.org/10.4462/annbotrm-13181>.
- Hardegree, S.P. and Emmerich, W.E. (1994) "Seed germination response to polyethylene glycol solution depth," *Seed Science and Technology*, 22, pp. 1–7.
- Heerden van, P.D.R., Swanepoel, J.W. and Kruger, G.H.J. (2009) "Modulation of photosynthesis by drought in two desert scrub species exhibiting C3 – mode CO<sub>2</sub> assimilation," *Environmental and Experimental Botany*, 61(2), pp. 124–136. Available at: <https://doi.org/10.1016/j.envexpbot.2007.05.005>.
- Kalachanis, D. and Manetas, Y. (2010) "Analysis of fast chlorophyll fluorescence rise (O-K-J-I-P) curves in green fruits indicates electron flow limitations at the donor side of PSII and the acceptor sides of both photosystems," *Physiologia Plantarum*, 139, pp. 313–323. Available at: <https://doi.org/10.1111/j.1399-3054.2010.01362.x>.
- Kalaji, H.M. *et al.* (2012) "Fluorescence parameters as early indicators of light fluorescence transient," *Journal of Photochemistry and Photobiology. B: Biology*, 104, pp. 236–257. Available at: <https://doi.org/10.1016/j.jphotobiol.2012.03.009>.
- Kalaji, H.M. *et al.* (2016) "Chlorophyll *a* fluorescence as a tool to monitor physiological status of plants under abiotic stress conditions," *Acta Physiologiae Plantarum*, 38, 102. Available at: <https://doi.org/10.1007/s11738-016-2113-y>.
- Kosmala, A. *et al.* (2012) "Changes in the chloroplast proteome following water deficit and subsequent watering in a high and a low drought tolerant genotype of *Festuca arundinacea*," *Journal of Experimental Botany*, 63, pp. 6161–6172. Available at: <https://doi.org/10.1093/jxb/ers265>.
- Lawson, T. *et al.* (2003) "The responses of guard and mesophyll cell photosynthesis to CO<sub>2</sub>, O<sub>2</sub>, light, and water stress in a range of species are similar," *Journal of Experimental Botany*, 54, pp. 1743–1752. Available at: <https://doi.org/10.1093/jxb/erg186>.
- Li, R. *et al.* (2006) "Evaluation of chlorophyll content and fluorescence parameters as indicators of drought tolerance in barley," *Agricultural Sciences in China*, 5, pp. 751–757. Available at: [https://doi.org/10.1016/S1671-2927\(06\)60120-X](https://doi.org/10.1016/S1671-2927(06)60120-X).
- Mastalerczuk, G., Borawska-Jarmułowicz, B. and Kalaji, H.M. (2017) "Response of Kentucky bluegrass lawn plants to drought stress at early growth stages," *Pakistan Journal of Agricultural Sciences*, 54, pp. 811–817. Available at: <https://doi.org/10.21162/PAKJAS/17.5232>.
- Mehta, P. *et al.* (2010) "Chlorophyll *a* fluorescence study revealing effects of high salt stress on PSII in wheat leaves," *Plant Physiology and Biochemistry*, 48, pp. 16–20. Available at: <https://doi.org/10.1016/j.plaphy.2009.10.006>.
- Omar, S.A. *et al.* (2018) "Over expression of *Jatropha's* dehydrin jcdhn-2 enhances tolerance to water stress in rice plants," *International Journal of Biosciences*, 13, 2, pp. 53–65. Available at: <https://doi.org/10.31031/EAES.2018.03.000563>.
- Oukarroum, A. *et al.* (2007) "Probing the responses of barley cultivars (*Hordeum vulgare* L.) by chlorophyll *a* fluorescence OLKJIP under drought stress and re-watering," *Environmental and Experimental Botany*, 60, pp. 438–446. Available at: <https://doi.org/10.1016/j.envexpbot.2007.01.002>.
- Perlikowski, D. *et al.* (2016) "Remodeling of leaf cellular glycerolipid composition under drought and re-hydration conditions in grasses from the *Lolium-Festuca* complex," *Frontiers in Plant Science*, 7, 1027. Available at: <https://doi.org/10.3389/fpls.2016.01027>.
- Schansker, G., Toth, S.Z. and Strasser, R.J. (2005) "Methylviologen and dibromothymoquinone treatments of pea leaves reveal the role of photosystem I in the Chl *a* fluorescence rise OJIP," *Biochimica et Biophysica Acta*, 1706, pp. 250–261. Available at: <https://doi.org/10.1016/j.bbabi.2004.11.006>.
- Slabbert, R.M. and Krüger, G.H.J. (2011) "Assessment of changes in photosystem II structure and function as affected by water deficit in *Amaranthus hypochondriacus* L. and *Amaranthus hybridus* L.," *Plant Physiology and Biochemistry*, 49, pp. 978–984. Available at: <https://doi.org/10.1016/j.plaphy.2011.05.001>.
- Sousa de, C.A.F. *et al.* (2017) "A procedure for maize genotypes discrimination to drought by chlorophyll fluorescence imaging rapid light curves," *Plant Methods*, 13, 61. Available at: <https://doi.org/10.1186/s13007-017-0209-z>.
- Staniak, M. and Kocoń, A. (2015) "Forage grasses under drought stress in conditions of Poland," *Acta Physiologiae Plantarum*, 37, 116. Available at: <https://doi.org/10.1007/s11738-015-1864-1>.
- Stirbet, A. and Govindjee (2011) "On the relation between the Kautsky effect (chlorophyll *a* fluorescence induction) and photosystem II: Basics and applications of the OJIP fluorescence transient," *Journal of Photochemistry and Photobiology. B: Biology*, 104, pp. 236–257. Available at: <https://doi.org/10.1016/j.jphotobiol.2010.12.010>.
- Stirbet, A. and Govindjee (2012) "Chlorophyll *a* fluorescence induction: A personal perspective of the thermal phase, the J-I-P rise," *Photosynthesis Research*, 113, pp. 15–61. Available at: <https://doi.org/10.1007/s11120-012-9754-5>.
- Strasser, R.J. *et al.* (2010) "Simultaneous in vivo recording of prompt and delayed fluorescence and 820-nm reflection changes during drying and after rehydration of the resurrection plant *Haberlea rhodopensis*," *Biochimica et Biophysica Acta Bioenergetics*, 1797, pp. 1313–1326. Available at: <https://doi.org/10.1016/j.bbabi.2010.03.008>.
- Strasser, R.J., Srivastava, A. and Tsimilli-Michael, M. (2000) "The fluorescent transient as a tool to characterize and screen photosynthetic samples," in M. Yunus, U. Pathre and P. Mohanty (eds.) *Probing photosynthesis: Mechanisms, regulation and adaptation*. London: Taylor and Francis, pp. 445–483. Available at: <https://ppsystems.com/wp-content/uploads/the-fluorescence-transient.pdf> (Accessed: September 08, 2023).
- Strasser, R.J., Tsimilli-Michael, M. and Srivastava, A. (2004) "Analysis of the chlorophyll *a* fluorescence transient," in G.C. Papageorgiou and Govindjee (eds.) *Chlorophyll fluorescence: A signature of photosynthesis*. Dordrecht: Springer, pp. 321–362. Available at: [https://doi.org/10.1007/978-1-4020-3218-9\\_12](https://doi.org/10.1007/978-1-4020-3218-9_12).
- Tsimilli-Michael, M. (2020) "Revisiting JIP-test: An educative review on concepts, assumptions, approximations, definitions and terminology," *Photosynthetica*, 58 (SI), pp. 275–292. Available at: <https://doi.org/10.32615/ps.2019.150>.
- Živčák, M. *et al.* (2008) "Performance index as a sensitive indicator of water stress in *Triticum aestivum* L.," *Plant Soil Environment*, 54, pp. 133–139. Available at: <https://doi.org/10.17221/392-PSE>.
- Živčák, M. *et al.* (2013) "Photosynthetic electron transport and specific photoprotective responses in wheat leaves under drought stress," *Photosynthesis Research*, 117, pp. 529–546. Available at: <https://doi.org/10.1007/s11120-013-9885-3>.